

Revisiting the fold discontinuity after ACCP binning

Xinxiang Li and Han-xing Lu

ABSTRACT

In converted wave seismic data processing, common conversion point (CCP) binning and stacking is commonly used to transform the converted wave data into a different domain where many conventional pure-mode seismic data processing procedures can be more conveniently applied. However, because CCP binning requires velocity information, which is often not available with desired accuracy, a simplified method called asymptotic common conversion point (ACCP) binning is often used. The ACCP binning process usually requires only a value of the P-wave and S-wave velocity ratio. It is noticed that, after ACCP binning with the original CMP spacing as in pure-mode data processing, the CCP fold distribution often has periodical discontinuities. This discontinuity may result in spatial inconsistency on the CCP stacked sections, and then influences the quality of final migration and interpretation.

Starting from analysing the CMP and CCP fold distributions of single-shot acquisition geometry, the reasons of the CCP fold discontinuity are revisited in this paper. The main reason of CCP fold discontinuity can be explained as that the CCP coverage of each one-shot-multi-receiver experiment is larger than the CMP coverage. According to this fold discontinuity problem, the optimum bin-width concept is also involved. The optimum bin-width is not only dependent to the acquisition geometry, it also depends on the effective P-wave and S-wave velocity ratio used for the ACCP binning. The optimum bin-width is usually larger than the CMP spacing, which is determined directly by the acquisition geometry. Some practical approaches to overcome the fold-discontinuity problem are also discussed.

INTRODUCTION

Eaton and Lawton (1992) discuss the problem of the periodical discontinuity of ACCP fold distribution when converted wave data is binned with original CMP spacing. The fold discontinuity may result in lateral inconsistency along the reflection events on CCP stacked sections. With acquisition geometry surface map and stacking charts, Eaton and Lawton (1992) present a clear graphic explanation how the fold discontinuity happens. More importantly, they also found that a specific ACCP bin-width dependent to the P-wave to S-wave velocity ratio (shortened as V_P/V_S ratio) could essentially solve the fold-discontinuity problem. In Lawton (1993), this specific bin-width is called optimum bin size, and will also be discussed later in this paper. In practice, the fold discontinuity problem may be partly solved by increasing the bin width used for ACCP binning. For example, an ACCP bin-width twice the CMP spacing can result in CCP stacked sections with much better spatial consistency (Eaton and Lawton, 1992).

In this paper, the ACCP fold discontinuity problem will be explained in terms of some typical acquisition geometry, and will be analyzed through a variety of numerical experiments. In conjunction with Eaton and Lawton's findings (1992), our

results reveal that the fold discontinuity problem will not be solved by arbitrarily increasing the CCP bin size. To essentially eliminate the CCP fold discontinuity, the optimum bin size (and its multiples) should be used.

ASYMPTOTIC CONVERSION POINT

For simplicity, it is supposed that there is only one flat reflector (at depth Z) in the subsurface, and the material between the surface and the reflector is homogeneous with P-wave velocity V_P and shear wave velocity V_S , as shown in Figure 1. The V_P/V_S ratio is denoted as γ and, for convenience, the V_S to V_P ratio is denoted as γ' . If the waves start at the source location **S** as P-waves and arrive at location **C** on the reflector with an incident angle of θ_P , then convert into S-waves and reflect back to the receiver location **R** with a reflection angle θ_S , Snell's law can be written as

$$\frac{\sin(\theta_P)}{V_P} = \frac{\sin(\theta_S)}{V_S} \quad (1)$$

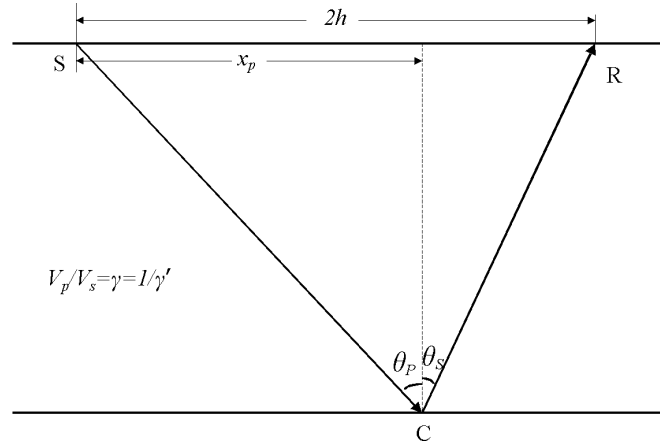


Figure 1: Ray path of P-S conversion at one subsurface reflector.

In Figure 1, the horizontal distance between the source location **S** and the conversion point **C** is denoted as x_p , and the source-receiver offset is denoted as $2h$, the following equations hold:

$$\tan(\theta_P) = \frac{x_p}{Z} \quad (2a)$$

$$\tan(\theta_S) = \frac{2h - x_p}{Z} \quad (2b)$$

Keeping in mind that both θ_P and θ_S tend to 0 as the depth of the reflector, Z , tends to infinity, dividing (2a) with (2b) results in

$$\frac{x_p}{2h - x_p} = \frac{\tan(\theta_P)}{\tan(\theta_S)} = \frac{\sin(\theta_P)}{\sin(\theta_S)} \cdot \frac{\cos(\theta_S)}{\cos(\theta_P)} = \frac{V_p}{V_s} \cdot \frac{\cos(\theta_S)}{\cos(\theta_P)} \xrightarrow{z \rightarrow \infty} \frac{V_p}{V_s} = \gamma \quad (3)$$

and then

$$x_p \approx \frac{2h\gamma}{1 + \gamma} = \frac{2h}{1 + \gamma'} \quad (4)$$

Expression (4) indicates the asymptotic location of the conversion point, which is determined by the source-receiver offset and the V_p/V_s ratio. The asymptotic conversion points calculated from expression (4) are often used to form common conversion point (CCP) gathers, and this process of binning traces into CCP gathers is called asymptotic CCP binning or abbreviated as ACCP binning. The ACCP binning is not accurate because, firstly, it does not depend on the accurate locations of the conversion points (we almost never know where they are), and secondly, it is known that the conversion points change their lateral locations with depth. However, years of practical applications demonstrate that ACCP binning is one of the most powerful techniques in converted wave seismic data processing, even though many more accurate, time-variant binning techniques have shown their necessity.

ACCP FOLD DISTRIBUTION

Figure 2 is a simple diagram of a single-shot geometry with ray paths shown for P-wave to P-wave reflections (light grey color) and asymptotic P-wave to S-wave reflections (dark color).

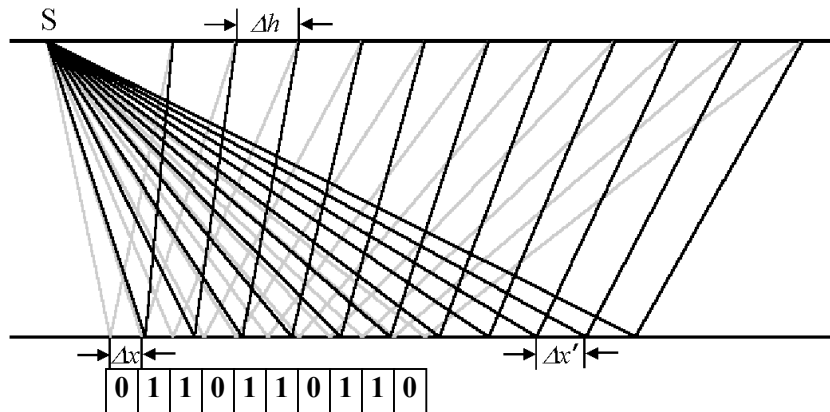


Figure 2: Single-shot geometry with PP and asymptotic PS reflection ray paths. '0' and '1' indicate the number of the asymptotic conversion points falling in the original CMP bins.

If the receiver interval is denoted as Δh , then the CMP spacing is $\Delta x = 0.5\Delta h$. Taking two adjacent receiver locations with offset h_1 and h_2 , i.e., $h_2 - h_1 = \Delta h$, the asymptotic CCP locations (identified as the distances from the same source location) are

$$x_{p1} = \frac{h_1}{1 + \gamma'} \text{ and } x_{p2} = \frac{h_2}{1 + \gamma'} \quad (5)$$

Therefore, the CCP spacing between these two traces is

$$\Delta x' = x_{p2} - x_{p1} = \frac{h_2 - h_1}{1 + \gamma'} = \frac{2}{1 + \gamma'} \Delta x \quad (6)$$

In practice, the V_p/V_s ratio used for asymptotic binning is usually fixed for the whole data set. The independence of $\Delta x'$ to the offset values, h_1 and h_2 , implies that all the asymptotic conversion points in the single-shot geometry are evenly spaced, just like CMP locations. Therefore, some fixed bin-sizes ($\Delta x'$ itself, e.g.) for ACCP binning should result in continuous fold distribution. The CCP binning with bin size of $\Delta x'$ is called the optimum bin size (Lawton, 1993).

If the CMP spacing is used as the ACCP bin size, the CCP fold distribution of the single-shot experiment in Figure 2 will result in (as listed in the figure).

0 1 1 0 1 1 0 1 1 0

This can be verified by simply counting the number of ACCP points in each CMP bins starting from the first CMP location and stopping at the last CMP location. The '0's between '1's show the fold discontinuity.

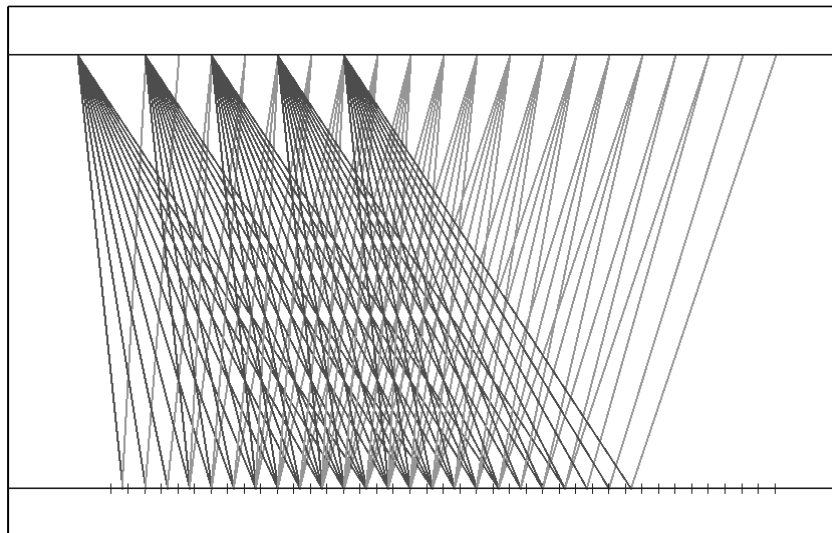


Figure 3: The ray-path geometry of asymptotic PS reflection with 5-shot geometry, where the shot spacing is twice the receiver spacing. The down-going waves are plotted with a darker color than the up-coming waves.

One might expect that this ACCP fold discontinuity to disappear when multi-shot experiments are considered as in the real world. Unfortunately, this is not the case. The ray-path diagram in Figure 3 shows a multi-shot example of ACCP fold discontinuities in terms of using CMP bin-size. The little ticks indicate the CMP locations. The following series of numbers is the result of counting the number of asymptotic conversion points in each CMP interval,

1 1 0 1 2 2 0 2 3 3 0 3 4 4 0 4 4 4 0 4 3 3 0 3 2 2 0 2 1 1 0 1

The discontinuity of this distribution is obvious and the periodicity is shown by that every two zero-fold ACCP locations have three non-zero-fold ACCP locations in between.

Eaton and Lawton (1992) give an explanation for this periodical discontinuity using surface stacking chart, which is valid for general 2D acquisition geometries. In fact, this problem exists even for 3D ACCP fold (1993, Lawton).

The fold discontinuity is the result of using CMP spacing as the ACCP bin size. The reason of using CMP spacing as the bin size is mainly for creating final stack sections with trace spacing equal to conventional pure-mode (P-P) stack sections. But unfortunately, CMP spacing is not an appropriate choice for ACCP binning.

Because of the mode conversion, the CMP coverage (the lateral range covered by all CMP locations) and the ACCP coverage (the horizontal range covered by all ACCP locations) are different. In the one-shot experiment as shown in Figure 2, the 11 receivers result in 11 CMP locations and 11 CCP locations. The distance between the last and the first (the coverage) CMP locations is $10\Delta x$, while the ACCP coverage is $10\Delta x'$, and it is $2/(1+\gamma')$ (which should always greater than 1) times of the CMP coverage. The CMP coverage and the CCP coverage share the same number of traces, implying that the CCP spacing should be $2/(1+\gamma')$ times of the original CMP spacing, which is, again, $\Delta x'$.

In terms of resolution, it is not reasonable to expect the same number of samples with a larger sample rate, which have larger coverage, have the same resolution. That is to say, even the converted wave data can be binned with a smaller bin-size than $\Delta x'$, (Δx , e.g.) the results do not provide any higher resolution. Instead, the results can be similarly obtained by an interpolation after binning with bin size $\Delta x'$.

SOME NUMERICAL EXPERIMENTS

Some results on the ACCP fold distribution are obtained from numerical experiments with different ACCP bin sizes and different acquisition geometries. For all the experiments, the following acquisition geometry parameters are the same:

total number of shots: 10
 number of receivers: 48
 nearest offset: 100 m
 receiver interval: 25 m.

Different experiments have different values of shot interval, which is given as times of corresponding receiver intervals. In each acquisition geometry, different V_P/V_S ratios and different bin sizes may be used. For simplicity, these experiments use one-side spreading for all the shots, which may only be suitable for conventional marine acquisition.

EXPERIMENT 1: the shot interval is twice the receiver interval

In this experiment, different results are shown with different ACCP binning parameters: the V_p/V_s ratio γ , and the ACCP bin size Δw .

$\gamma = 2$, $\Delta w = \Delta x$, the CMP spacing

Conventional ACCP binning uses bin size equal to the CMP spacing. With $\Delta w = \Delta x$ and a V_p/V_s ratio of 2, the ACCP fold on the experimental geometry is shown in Figure 4 (in dark colour). In comparison, the CMP fold distribution is also shown in grey. The periodical discontinuity of the ACCP fold is evident.

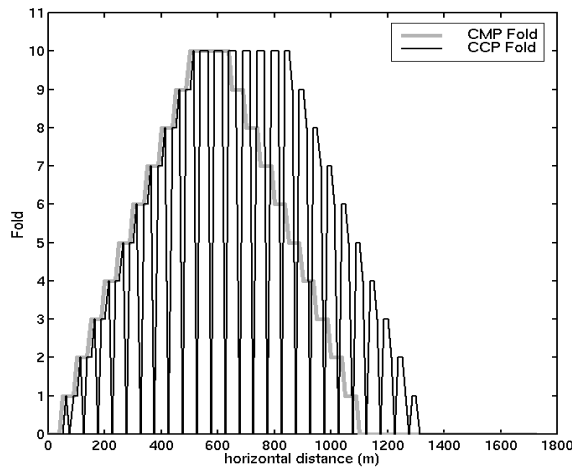


Figure 4: ACCP fold (black) and CMP fold (grey) with $\gamma = 2$, $\Delta w = \Delta x$ for the geometry with the shot spacing twice the receiver interval.

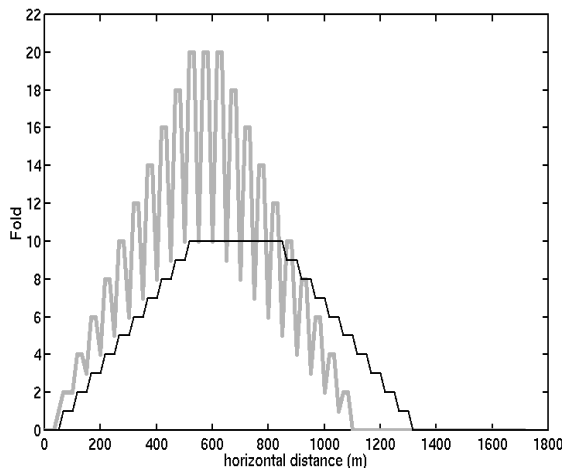


Figure 5: ACCP fold (black) and CMP fold (grey) with $\gamma = 2$, $\Delta w = 2\Delta x/(1+1/\gamma)$ for the geometry with the shot spacing twice the receiver interval.

$\gamma = 2$, $\Delta w = 2\Delta x/(1+1/\gamma)$, the optimum bin size

With the same V_p/V_s ratio, which is a parameter determined upon the subsurface formation instead of the acquisition geometry, and with the optimum ACCP bin size, $2\Delta x/(1+1/\gamma)$, the resultant ACCP fold is continuous. This ACCP fold is displayed in

Figure 5 in black colour and the CMP fold with this new bin-size is shown in grey. By similar reason for the ACCP fold in Figure 4, the new CMP fold becomes periodically discontinuous.

$\gamma = 2$, and $\Delta w = 2\Delta x$, the receiver interval

The ACCP fold (black) and CMP fold (grey) with $\gamma = 2$ and $\Delta w = 2\Delta x$ are shown in Figure 6. It can be seen that, when the ACCP bin size becomes larger, i.e. $2\Delta x > 2\Delta x/(1+1/\gamma)$, the ACCP fold discontinuity may appear again, although the discontinuity is relatively less serious than that in the case using the original CMP spacing.

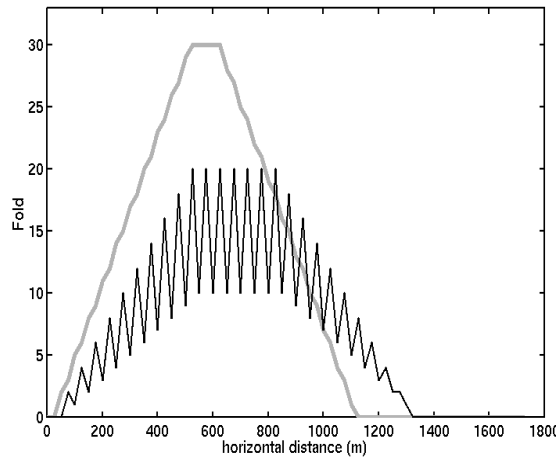


Figure 6: ACCP fold (black) and CMP fold (grey) with $\gamma = 2$, $\Delta w = 2\Delta x$ for the geometry with the shot spacing twice the receiver interval.

The differential of a fold distribution at a horizontal location is defined as the difference of the fold value at the next location and the present location. It can be used as a quantity indicator of the significance of the discontinuity of relevant fold distribution. When the absolute value of a fold differential function is larger, it can generally be considered that the fold distribution is more discontinuous. Figure 7 shows three ACCP fold differentials corresponding to the ACCP fold functions shown in Figure 4, Figure 5, and Figure 6.

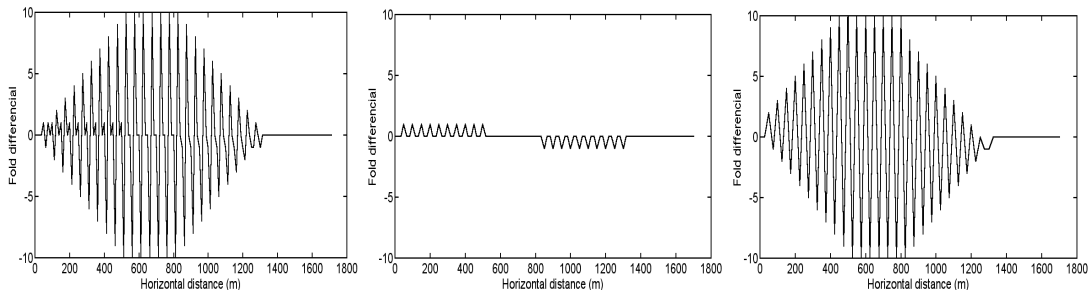


Figure 7: (a), (b), and (c) are the differentials of the ACCP fold distributions in Figures 4, 5, and 6, respectively.

From Figure 7, it can be seen that the ACCP fold with the bin size of $2\Delta x/(1+1/\gamma)$ (shown in Figure 5) has the best continuity. The differentials of the ACCP folds in

Figures 4 and 6 are very close, although the ACCP fold discontinuity in Figure 6 (no zero fold ACCP location in the middle of the coverage) may not be as bad, relatively speaking, as the fold in Figure 4.

$$\gamma = 3.5, \Delta w = \Delta x$$

The following results are obtained based on the same acquisition geometry as above experiments, but for another area where the V_p/V_s ratio for ACCP is chosen as 3.5. Again, the original CMP spacing is first used for ACCP binning, as expected, the ACCP fold is again periodically discontinuous (shown as black lines in Figure 8). It is worth noting that the discontinuity of the fold distribution is not as serious as in Figure 4, and that the only difference between these two fold results is that different V_p/V_s ratios have been used for the ACCP binnings, i.e., 2 for Figure 4, and 3.5 for Figure 8.

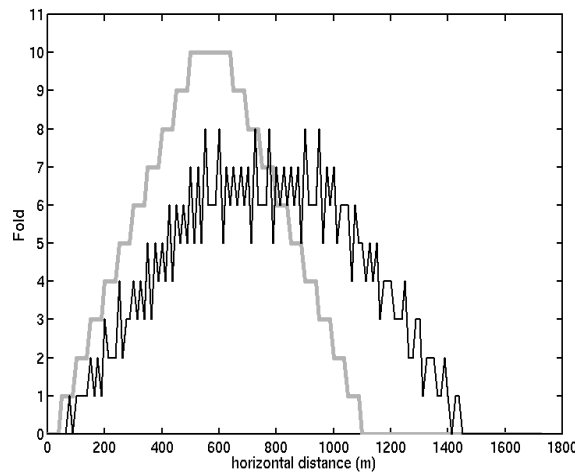


Figure 8: ACCP fold (black) and CMP fold (grey) with $\gamma = 3.5, \Delta w = \Delta x$ for the geometry with the shot spacing twice the receiver interval.

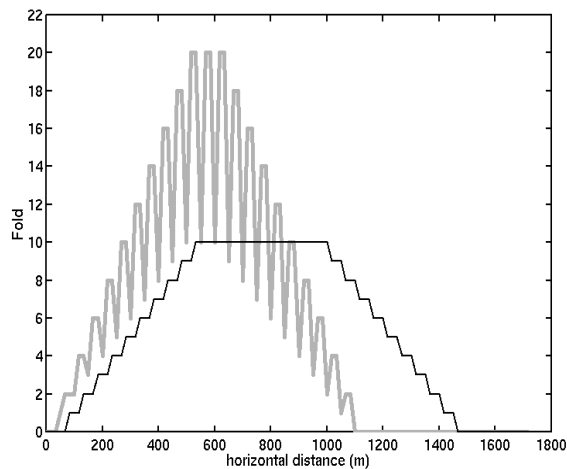


Figure 9: ACCP fold (black) and CMP fold (grey) with $\gamma = 3.5, \Delta w = 2\Delta x/(1+1/\gamma)$ for the geometry with the shot spacing twice the receiver interval.

$$\gamma = 3.5, \Delta w = 2\Delta x / (1 + 1/\gamma)$$

Figure 9 shows the fold distributions of the CMP and ACCP binnings with the optimum bin size, $2\Delta x / (1 + 1/\gamma)$. The ACCP fold is perfectly continuous.

$$\gamma = 3.5, \Delta w = 2\Delta x$$

Figure 10 shows the CMP fold (grey) and ACCP fold (black) with ACCP binning using bin size equal to $2\Delta x$. The ACCP fold continuity is relatively better comparing with the results in Figure 8. In Figure 10, most of the differences between two adjacent ACCP locations are 0 or 1, whereas in Figure 8, the differences were 2 or 3 for most locations.

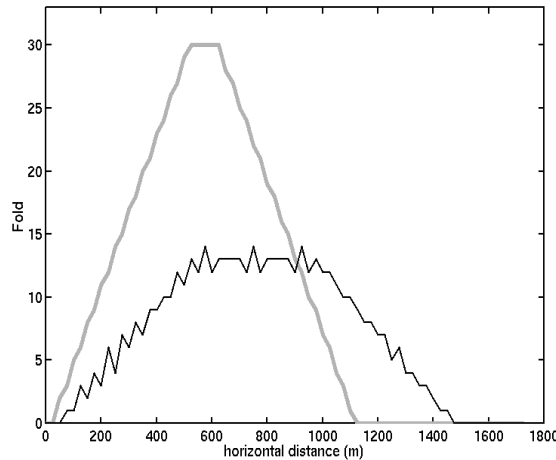


Figure 10: ACCP fold (black) and CMP fold (grey) with $\gamma = 3.5, \Delta w = 2\Delta x$ for the geometry with the shot spacing twice the receiver interval.

The fold differentials of the results in Figures 8, 9, and 10 are shown in Figure 11 (a), (b) and (c). The ACCP binnings with a V_p/V_s ratio of 3.5 provide much more stable ACCP fold distributions (Figure 11) than those with a V_p/V_s ratio of 2 (Figure 7) for both bin sizes of Δx and $2\Delta x$. This is because the shot interval as an integer multiple of the receiver interval is equal to the V_p/V_s ratio used for ACCP binning in Figure 4. In Figure 8, however, the shot interval is still twice the receiver interval but the V_p/V_s for binning is 3.5. More discussions on this relationship between shot interval, receiver interval and V_p/V_s ratio can be found in Eaton and Lawton (1992) and Lawton (1993).

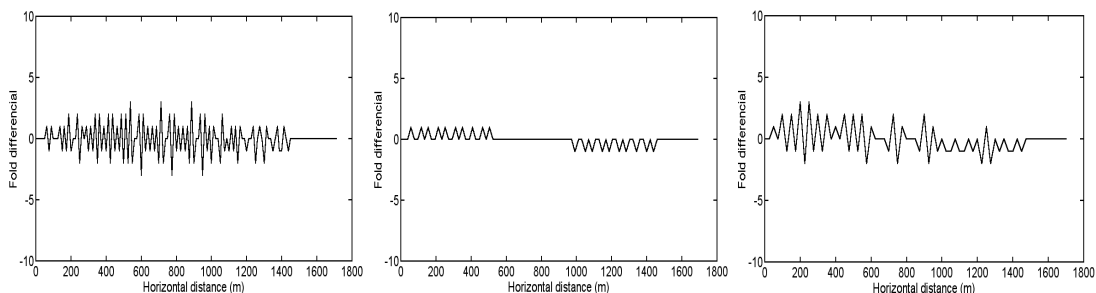


Figure 11: (a), (b), and (c) are the differentials of the ACCP fold distributions in Figure 8, Figure 9, and Figure 10 respectively.

EXPERIMENT 2: the shot interval is 3 times the receiver interval

In this experiment, the V_P/V_S ratio γ is fixed at 2, and different ACCP bin size, Δw , are used.

Figure 12 shows the CMP fold (grey) and ACCP fold (black) using CMP spacing Δx as the ACCP bin size. The ratio of shot-interval to receiver-interval, 3, is not an integer multiple of the V_P/V_S ratio, 2, so the expected ACCP fold should not contain zero-fold locations as it does in Figure 4. However, the fold is still seriously inconsistent.

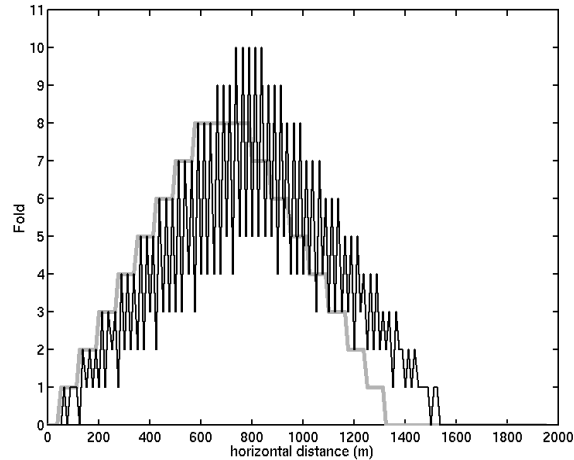


Figure 12: ACCP fold (black) and CMP fold (grey) with $\gamma = 2.0$, $\Delta w = \Delta x$ for the geometry with the shot interval is 3 times of the receiver interval.

Figure 13 shows the consistent ACCP fold distribution when the optimum bin size $2\Delta x/(1+1/\gamma)$ is used.

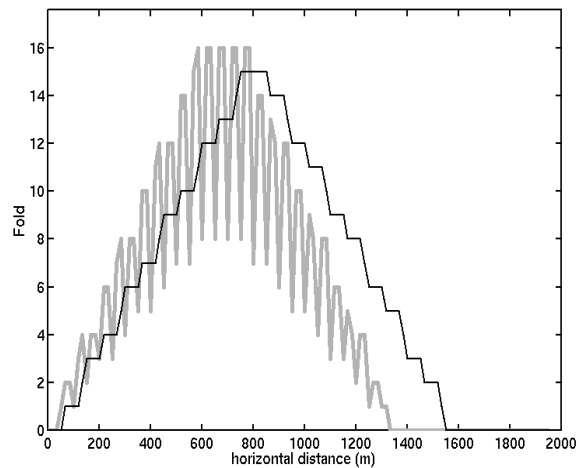


Figure 13: ACCP fold (black) and CMP fold (grey) with $\gamma = 2.0$, $\Delta w = 2\Delta x/(1+1/\gamma)$ for the geometry with the shot interval is 3 times of the receiver interval.

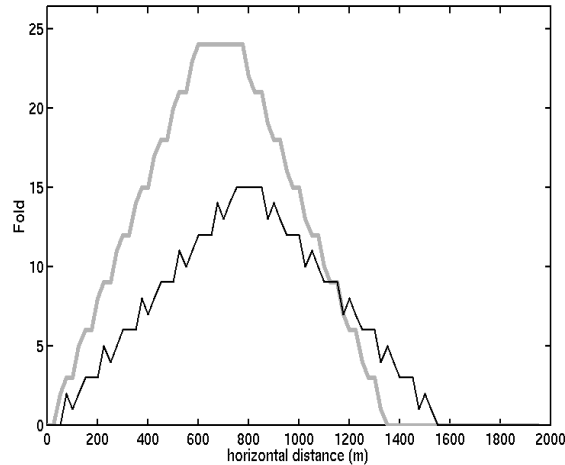


Figure 14: ACCP fold (black) and CMP fold (grey) with $\gamma = 2.0$, $\Delta w = 2\Delta x$ for the geometry with the shot interval is 3 times of the receiver interval.

Figure 14 shows the fold distributions using the receiver interval as the ACCP bin size. The ACCP fold is more consistent than the one in Figure 12. The maximum differential (absolute value) is only 2. Figure 15 shows the fold differential functions for the ACCP folds in Figures 12, 13 and 14, respectively.

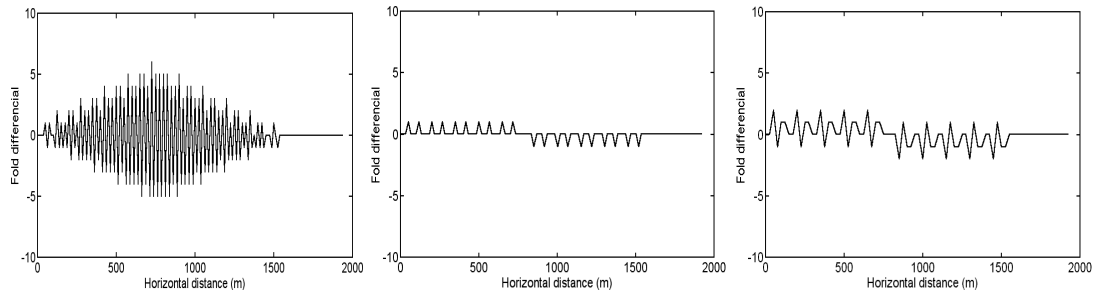


Figure 15: (a), (b), and (c) are the fold differential functions for the ACCP folds in Figures 12, 13 and 14, respectively.

EXPERIMENT 3: Small differences between V_p/V_s ratios

In this experiment, some "surprising" results with small differences in V_p/V_s ratios are shown. These results indicate that when the V_p/V_s ratio changes slightly, the resultant ACCP fold may have very different distributions. This implies the possibility of a "pure" practical technique to overcome the fold-discontinuity problem of ACCP binning. The results are obtained by using the same shot interval, which is twice the receiver interval, and the same ACCP bin size, which is the CMP spacing.

Figure 16 (a) shows the ACCP fold distribution with V_p/V_s ratio of 1.8, and the CMP fold is shown as a comparison. Figure 16 (b) shows the ACCP fold with V_p/V_s ratio of 2.2. The difference between these two ACCP fold distributions and the one shown in Figure 4 lies in their fold differentials. As shown in Figure 17, the fold differentials of the two fold distributions in Figure 16 are much smaller (3 to 10) than the one shown in Figure 7(a).

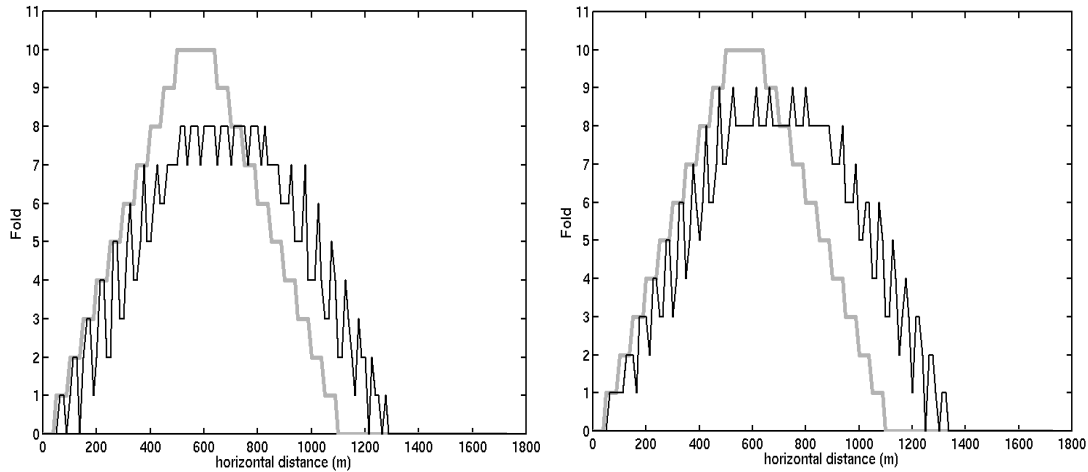


Figure 16: (a) ACCP fold with $\gamma=1.8$ and (b) ACCP fold with $\gamma=2.2$. The other parameters are all the same as the ones used for Figure 4.

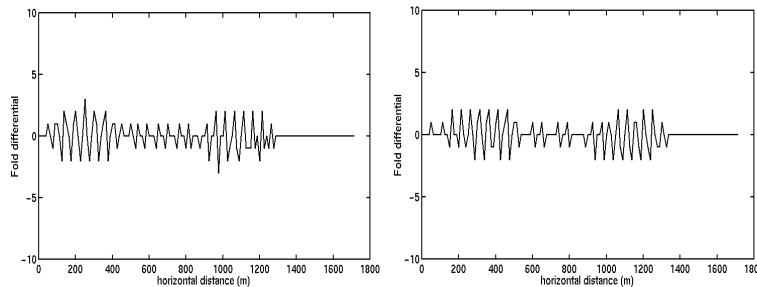


Figure 17: (a) and (b) are the fold differentials for the ACCP folds shown in Figure 16 (a) and (b) respectively.

BLACKFOOT DATA EXAMPLE

An experiment is also carried out using the Blackfoot III (1997) 2D 20 m radial component data. The shot and receiver intervals are the same in the acquisition of this dataset. The original CMP fold, as shown in Figure 18 (a), is perfectly consistent.

In the experiment, the V_p/V_s ratio of 2.0 was selected for this dataset. The ACCP binning with bin size of 10 m (the CMP spacing) resulted in an ACCP fold as shown in Figure 18 (b). The absolute differential values of this fold distribution are about 80 in the middle part of the line, which indicates a serious inconsistency. The ACCP binning with optimum bin size of 13.33 m resulted in a perfectly consistent fold distribution (Figure 18 (c)), as theoretically expected. As a practical comparison, ACCP binning with a V_p/V_s ratio of 1.9 and the original CMP bin size resulted in the fold distribution shown in Figure 18(d), which is much more consistent than the one with a V_p/V_s ratio of 2.0 (Figure 18(b)).

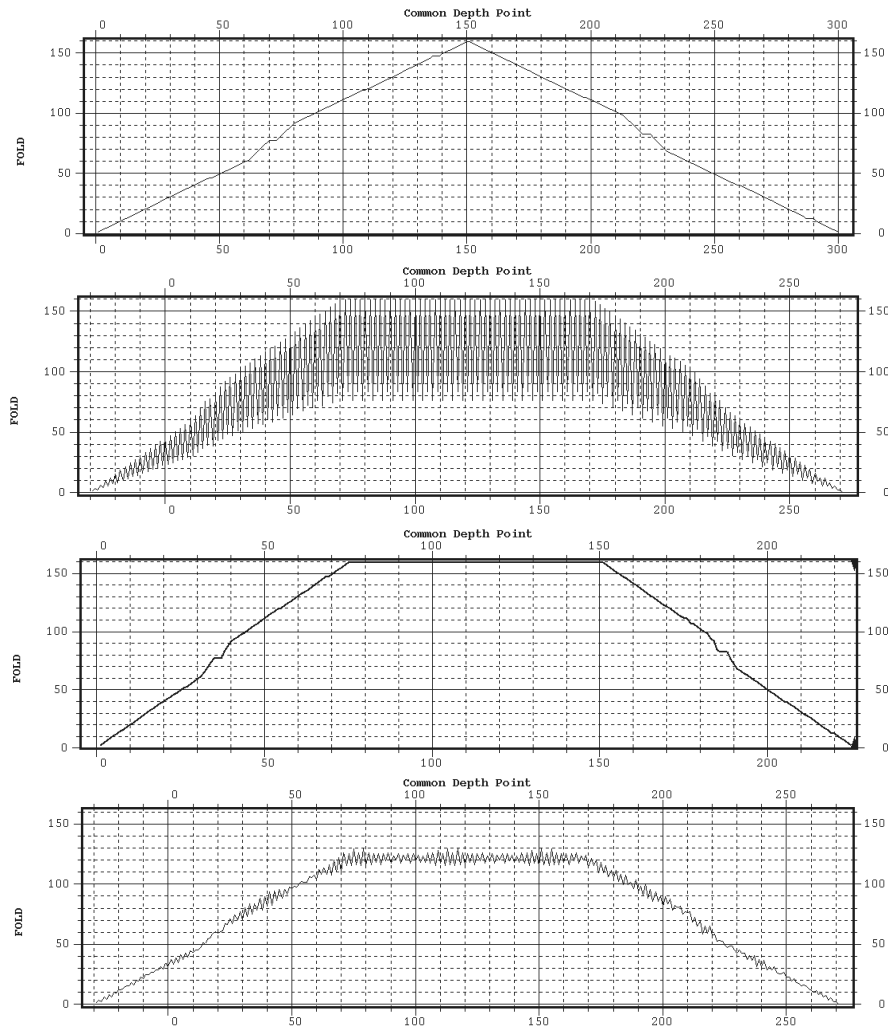


Figure 18: (a) original CMP fold; (b) ACCP fold using CMP spacing as the bin size and a V_p/V_s ratio of 2.0, (c) is the ACCP fold with optimum bin size ($V_p/V_s = 2.0$), and (d) the ACCP fold with original CMP bin size and V_p/V_s ratio of 1.9.

The Blackfoot dataset was stacked using different ACCP binning results. The stacked section shown in Figure 19 comes from the ACCP binning with fold distribution shown in Figure 18 (b). The stacked section shown in Figure 20 used the optimum bin size, and the number of the traces in this section is about 3/4 of the that of the section shown in Figure 19.

Perhaps because of the high fold of this dataset (minimum 80 for the middle part of Figure 18(b)), there is no evident visual difference between these two sections. However, along the events indicated by small white arrows in Figures 19 and 20, the continuity between 1500 to 2000 m is better on the section in Figure 20. This can be seen more clearly in the comparison between Figures 21 and 22, which are zoomed portions in the same time and horizontal limits of Figures 19 and 20.

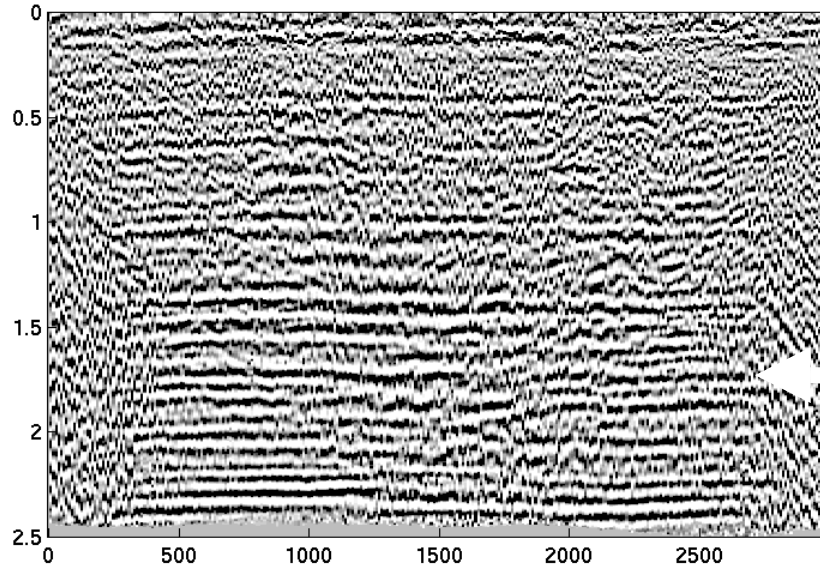


Figure 19: ACCP stacked section with the bin size same as the original CMP spacing

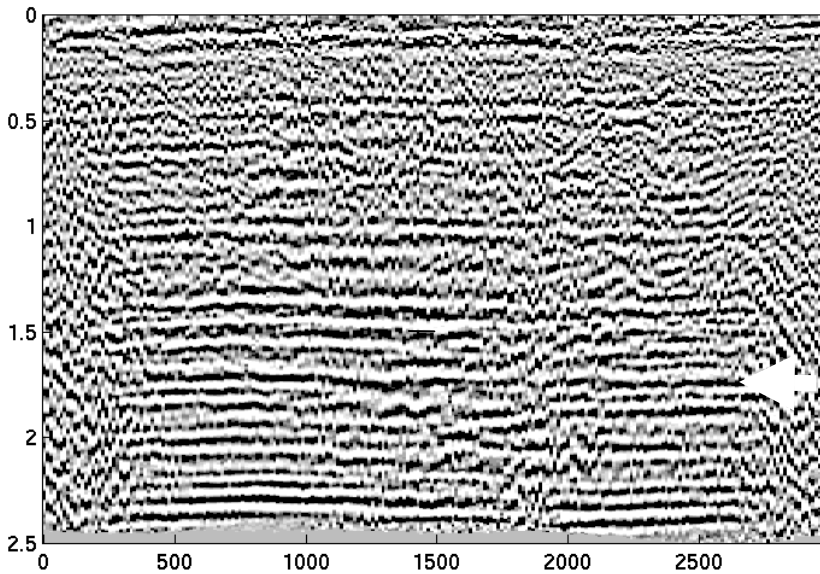


Figure 20: ACCP stacked section with the optimum bin size, which is $\frac{4}{3}$ of the original CMP spacing. The number of traces in this section is about $\frac{3}{4}$ of that in the section in Figure 19.

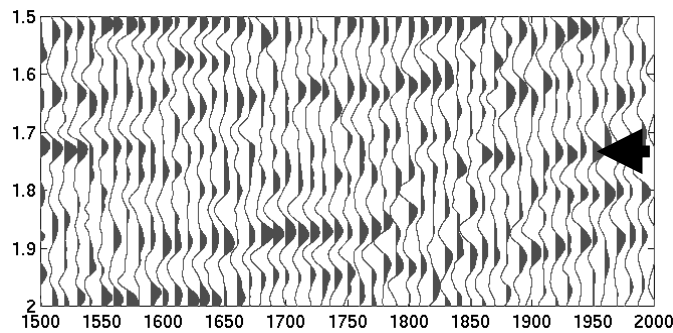


Figure 21: The portion of the stacked section shown in Figure 19 with time limit of 1.5 to 2.0 seconds and horizontal distance limit of 1500 to 2000 m.

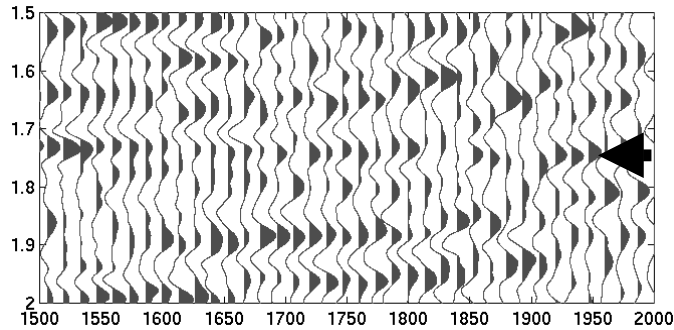


Figure 22: The portion of the stacked section shown in Figure 20 with time limit of 1.5 to 2.0 seconds and horizontal distance limit of 1500 to 2000 m. Again, the number of traces in this portion is about 3/4 of the number of traces shown in Figure 21.

The converted wave data sections are almost always used as assistant information for conventional P-P wave data sections. The P-P sections are usually displayed with trace spacing equal to the CMP spacing. A converted wave section with different trace spacing may involve difficulties for the comparisons with corresponding PP sections. This is why the ACCP binning process, as an important part of the converted wave seismic data processing, usually uses the CMP spacing as the bin size.

However, same trace spacing does not necessarily require the ACCP bin size to be the same. Eaton and Lawton (1992) show a section with trace spacing same as the CMP spacing but with larger bin size (the receiver interval), and this section shows enhancement of the horizontal consistency. The problem with a bin size larger than the bin (stacked trace) spacing is that the ACCP binning process may put one input trace into different bins. As a result, one trace may be stacked into different stacked traces. This is something similar to the stacked-trace interpolation or mixing.

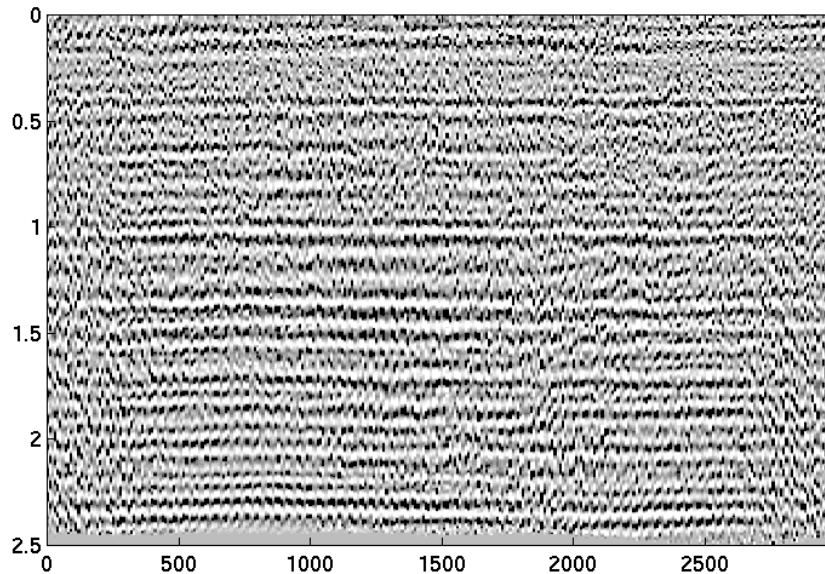


Figure 23: f-k interpolated section from the one shown in Figure 20. Its trace spacing is the same as that of the section shown in Figure 19.

Trace interpolation or mixing can be done after the ACCP binning with some larger bin size (such as the optimum bin size) and stacking. Figure 23 shows a section

obtained from the section (shown in Figure 20) by a 2D f-k interpolation. This section has the same trace spacing as the one shown in Figure 19. The events on this section show good consistency, although the section looks a little bit “foggy” due to some artefacts from the f-k interpolation.

SOFTWARE IMPLEMENTATION

The ACCP binning with different bin sizes has been implemented in ProMAX 2D. Comparing to the conventional ACCP binning module, called "P-Sv asymptotic binning" in ProMAX, the new binning module does not destroy the original CDP database or the CDP related header words. Therefore, after applying this new module, any CMP related processing can still be normally applied, even the old binning module itself. This is helpful because many prestack converted wave migration algorithms, such as $v(z)$ f-k migration, may use CDP information before the ACCP binning.

Simple geometry that, the total number of ACCP surface locations after binning with the optimum bin size should never exceed the total number of CMP locations. This property ensures that the whole ACCP information can be sufficiently saved in the CDP database without over-writing the CDP geometry.

CONCLUSIONS

The ACCP binning with original CMP spacing as the bin size results in spatial discontinuity in the ACCP fold distribution, which may result in event inconsistency on the stacked section (Eaton and Lawton, 1992). An optimum bin size (Lawton, 1993) that is dependent on the V_p/V_s ratio can essentially overcome this fold discontinuity problem. ACCP binning with appropriate bin size and trace interpolation after stacking may still provide converted wave sections conveniently comparable to conventional pure-mode P-P sections.

ACKNOWLEDGEMENTS

The authors would like to thank the sponsors of the CREWES Project for their financial support. We also thank Dr. Peter Cary for helpful and insightful suggestions. The help received from Ms. M. E. Cargan in the preparation of this paper is appreciated.

REFERENCES

- Eaton D.W.S. and Lawton, D.C., 1992, P-Sv stacking charts and binning periodicity: *Geophysics*, 57, 745-748.
- Lawton, D.C., 1993, Optimum bin size for converted wave 3-D asymptotic mapping, CREWES Research Report, Vol. 5, Ch. 28.